SAE International

2012-01-0569
Published 04/16/2012
doi:10.4271/2012-01-0569
saepcmech.saejournals.org

Assessment of the Simulated Injury Monitor (SIMon) in Analyzing Head Injuries in Pedestrian Crashes

Kyle A. Ott
Johns Hopkins Applied Physics Lab

John F. Wiechel
The Ohio State Univ.

Dennis A. Guenther
Ohio State Univ.

Jason Stammen
NHTSA

Ann E. Mallory
Transportation Research Center Inc.

ABSTRACT

Objectives. Examination of head injuries in the Pedestrian Crash Data Study (PCDS) indicates that many pedestrian head injuries are induced by a combination of head translation and rotation. The Simulated Injury Monitor (SIMon) is a computer algorithm that calculates both translational and rotational motion parameters relatable head injury. The objective of this study is to examine how effectively HIC and three SIMon correlates predict the presence of either their associated head injury or any serious head injury in pedestrian collisions.

Methods. Ten reconstructions of actual pedestrian crashes documented by the PCDS were conducted using a combination of MADYMO simulations and experimental headform impacts. Linear accelerations of the head corresponding to a nine-accelerometer array were calculated within the MADYMO model's head simulation. Injury risk calculated by SIMon (relative motion damage measure RMDM, cumulative strain damage measure CSDM, dilatation damage measure DDM) and HIC were compared to the presence or absence of either their associated injury or any serious head injury in each case using receiver operating characteristic (ROC) analysis.

Results. HIC (AUC = 0.91) and CSDM (AUC = 0.89) were both very effective at predicting their associated injury types (AIS 3+ skull fracture and DAI, respectively). DDM (AUC = 0.68) and RMDM (AUC = 0.56) were not as effective in predicting their respective injury types (contusion and acute subdural hematoma, respectively). However, HIC (AUC = 0.67) and CSDM (AUC = 0.62) were less effective than RMDM and DDM (AUC = 0.86 for both) for predicting any AIS 3+ head injury type.

Conclusions. For the ten cases evaluated in this study, each correlate was strong at predicting either its associated injury or any head injury. However, there was no single injury correlate that performed effectively in predicting both its associated injury and any AIS 3+ head injury. Because pedestrian head injuries are often associated with a combination of linear and rotational loading, supplementing HIC with correlates that capture other loading patterns could lead to more robust head injury assessment.

CITATION: Ott, K., Wiechel, J., Guenther, D., Stammen, J. et al., "Assessment of the Simulated Injury Monitor (SIMon) in Analyzing Head Injuries in Pedestrian Crashes," *SAE Int. J. Passeng. Cars - Mech. Syst.* 5(1):2012, doi: 10.4271/2012-01-0569.

INTRODUCTION

Pedestrian fatalities historically have accounted for more than 10 percent of traffic related fatalities each year in the United States. Of 37,261 traffic fatalities in 2008, 4,378 (11.7%) were pedestrians (NHTSA, 2009). Pedestrians account for an even larger percentage of fatalities in many other countries of the world. The majority of these deaths result from a head injury (Yoshida, 1999). In an effort to reduce pedestrian head injury, injury predictors that could estimate the risk of such severe and fatal injuries need to be examined.

The most commonly used criterion for determining the likelihood of head injury is the Head Injury Criterion (HIC). HIC is derived from the resultant translational acceleration measured at the center of gravity of a headform. This criterion was developed through the use of curve fitting analysis of the Wayne State Tolerance Curve (WSTC). This tolerance curve was developed from experiments that included impacts of dry human skulls, forehead impacts of embalmed cadavers and application of an air pressure pulse directly onto the dura of anesthetized animals (Lissner et al., 1960, Versace, 1971). Although HIC is calculated from only linear accelerations, it is a good indicator of skull fracture and has been used almost universally in crash injury research and head injury prevention since its introduction (IHRA, 2001). However, there have been several studies that indicate traumatic brain injury (TBI) is not only a function of linear acceleration but also rotational acceleration and the resulting strain within the brain itself (Hardy et al., 2001, Takhounts et al., 2003, Vorst et al., 2003). This evidence has created a need to investigate other criteria in the prediction of brain injury.

SIMon (Simulated Injury Monitor) is an injury-based model developed by the National Highway Traffic Safety Administration (NHTSA) and validated with both human and baboon experimental impact data (Takhounts et al., 2003). SIMon is designed to efficiently simulate an impact of up to 150 ms in duration. This model consists of a finite element replica of the skull and brain that includes a dura-cerebral spinal fluid (CSF) layer, brain, falx cerebri and bridging veins. It was originally intended to model the 50th percentile male human head and brain with a total mass of 4.7 kg but has since been adapted to other dummy sizes. In all, the model contains 10,475 nodes and 7,852 elements and was developed to predict the likelihood of diffuse axonal injuries (DAI), brain contusions, and acute subdural hematomas (ASDH). To determine the likelihood of each of these injuries, SIMon uses several different correlates to injury. Cumulative strain damage measure (CSDM) is a correlate for DAI based on the finding that this injury is associated with the cumulative volume of brain tissue experiencing tensile strains over a predefined critical level found from animal experiments (Abel et al., 1978, Meaney et al., 1993, Nusholtz et al., 1995, Stalnaker et al., 1977). Application of CSDM predicts a 50 percent probability of injury when 50 percent of the brain experiences a strain of 15 percent. Dilation damage measure (DDM) is a correlate for contusions and involves localized regions where stress in the brain results in negative pressures that are below values required to produce contusions. The pressure threshold is set at approximately −100 kPa (−14.7 psi), which corresponds to the vapor pressure of water, again established from animal impact tests (Nusholtz et al., 1995, Stalnaker et al., 1977). The spatial distribution of the volume reaching this negative pressure limit determines the likelihood of contusions. DDM predicts a 50 percent probability of injury when 7.2 percent of the brain achieves a pressure of −100kPa. Finally, the relative motion damage measure (RMDM) is a correlate for ASDH injuries. This correlate predicts the potential for failure of a bridging vein at any time by calculating the ratio of the current strain to the failure strain. RMDM predicts an 50 percent probability of injury when RMDM=1.0. SIMon is able to predict these three injuries by using linear acceleration data from the nine-accelerometer array-equipped dummy head (NAAH) (DiMasi, 1995) or six degree of freedom data consisting of linear accelerations and angular rates to derive the corresponding rotational components that have been shown to correlate with brain injury.

Cases simulated in the current study were based on pedestrian crashes documented in the Pedestrian Crash Data Study (PCDS). The study collected detailed crash information from 548 non-duplicate pedestrian accidents in six major U.S. cities between 1994 and 1998. The resulting database provides necessary vehicle and crash parameters required to reconstruct many of the cases.

Head injury cases in PCDS were analyzed to estimate the prevalence of rotational injury mechanisms in pedestrian head injuries. The analysis done for this study was based on the classification of head injuries developed by Martin (Peter Martin, personal communication) and used by Arbogast et al. (2005), which categorizes the mechanism of each AIS 2+ head injury code as translation only, rotation only, or attributable to either rotation or translation. Rotationally induced brain injuries were defined to include only those associated with diffuse axonal injuries (DAI) and deep inertial strains. Injuries that fall into the translational category include skull fractures as well as injuries to the vascular network in the brain. The rest of the brain injuries are classified as caused by either “rotation or translation”, including loss of consciousness (LOC) injuries without further detail. In the current analysis of head injuries in the PCDS database, each pedestrian's AIS 2-6 head injuries were then determined to be a result of one of these mechanisms exclusively or a combination of these mechanisms. Results showed that for the 168 pedestrians in the database with AIS 2-6 head injuries and the 114 pedestrians with AIS 3+ head injuries, those with exclusively rotational injuries slightly out-numbered those with only translational injuries. However, the majority of pedestrians sustained head injuries from a combination of both rotational and translational mechanisms (Figure 1), suggesting a need for head injury

criteria to evaluate the combined risk of rotational and translational loading in pedestrian impacts.

The objective of this study was to examine the effectiveness of the three SIMon correlates (DDM, CSDM, RMDM) and HIC in their identification of head injury in pedestrian collisions. To estimate the effectiveness of SIMon, ten pedestrian case reconstructions were conducted using a combined approach of MADYMO simulations and experimental headform impact tests. The head injury risks calculated by SIMon and HIC were compared to the presence or absence of either their associated head injury or any serious head injury in the actual case. The effectiveness of each correlate was examined quantitatively using receiver operating characteristic (ROC) analysis.

METHODS

CASE SELECTION

Ten cases were chosen from the PCDS database (Table 1) based on the requirements of having (1) a frontal impact and pedestrian head contact at some point on the front profile of the impact vehicle, (2) sufficient pedestrian and vehicle information in the case to complete a reconstruction, and (3) availability/access to the case-documented vehicle make/model to obtain experimental stiffness data from a head impact at the case-documented impact point. The MAIS value listed in Table 1 refers to the maximum AIS level of head injury that occurred for the given case. Note that 7 of the 10 cases had an AIS 3+ head injury of some type.

The vehicle impact speed confidence interval shown in Table 1 is an estimate of the accuracy of the vehicle speed reported in the PCDS case. The PCDS coding system only allows for specification of a range of the uncertainty of the vehicle speed and this range is reported in Table 1. For example, the estimated speed for case 3 is 40 km/h, with a confidence band between 2 and 8 km/h wide. Therefore, the upper bound is between 41 and 44 km/h, and the lower bound is between 39 and 36 km/h.

RECONSTRUCTION OF PEDESTRIAN HEAD IMPACT

The use of two applications of the MADYMO model in this analysis procedure indicates a need to present an overview of the method. For each individual case, an initial kinematic simulation in MADYMO was conducted based upon the recorded pedestrian size and vehicle geometry information from the PCDS data. The objective of this model was to obtain the impact velocity and impact angle of the head at first contact with the vehicle. A number of vehicle speed and pedestrian stance combinations were applied iteratively until the head impact location in the simulation was consistent with the case-documented head contact point. The calculated head impact velocity and approach angle were used as the experimental conditions for a component headform impact test. The head acceleration data from the component headform impact test was subsequently used to define the head-vehicle contact properties for a repeat MADYMO simulation. Finally, the nine-accelerometer head acceleration data obtained from the MADYMO model in the second set of simulations was used to calculate HIC and rotational injury correlates in SIMon.

Pedestrian Model: The pedestrian models used in each case were Hybrid III ellipsoid standing dummy models provided in MADYMO (50th percentile male, 5th percentile female and 6 year old child) scaled with MADYMO Scalar to match the height and weight characteristics of the pedestrian in each case. The Hybrid III was chosen due to its availability in multiple sizes. Validation of this model for lateral impact is presented in the discussion. The specific dummy model chosen for each case was determined by the similarity of the accident subject's characteristics to the available models (i.e., the 8 year old child was modeled with a scaled 5th percentile female). The dummy model was then scaled to the accident subject's height and weight. It is recognized that the Hybrid III dummy is not designed for lateral impact and the Hybrid III model has not been validated for lateral impact. To evaluate the suitability of using this particular model, the head velocity and trajectory of the male 50th percentile Hybrid III model were compared with the head velocity and trajectory in post-mortem human subject (PMHS) tests conducted by Ishikawa, et al (1993). This comparison of the simulated head velocities and the PMHS head impact velocities showed that the Hybrid III MADYMO pedestrian model gives reasonable head motion and provides the necessary validation of the model in pedestrian impact situations (Stammen, 2001). Since head injury is the main concern of this study, matching the head impact velocity of the model to published PMHS values was sufficient.

Vehicle Model Geometry: Digital mapping of surrogate vehicles of the same make and model as those in Table 1 was completed using a FARO arm (Model G1202 Rev. 4.6, FARO Technologies Inc., Lake Mary FL), a digital position-recording device. The front profile of each vehicle was mapped with a grid pattern of points, approximately 50 mm apart. This spacing changed around certain contours as appropriate in order to obtain the specific details of each profile. The resulting data points were imported into Hypermesh® (Version 6.0, Altair, Troy MI) and then integrated into a three-dimensional object for use in MADYMO. Due to the lack of availability of three of the ten vehicles (cases 1, 4, and 6), the profiles for those three vehicles were approximated using measurements provided from the PCDS documentation. For these vehicles, a combination of simplified cylinders and planes was used to approximate the striking vehicle's profile (i.e., planes for the hood, horizontal cylinder for the hood edge, plane for the grill, and planes and cylinders for the bumper). Since the case vehicle dimensions were well-defined in these three cases, the lack of digitized vehicle geometry was not expected to

significantly alter the pedestrian model's overall kinematics in the simulation.

Kinematic Simulation of Impact: The kinematic simulation of the impact was based on the reported vehicle impact speed, pedestrian stance and motion (running, jogging, walking, etc.) at impact, initial leg impact point documented on the case vehicle, head impact orientation based on superficial injuries to the head, WAD (Wrap-Around Distance), and lateral head impact location. The initial estimate of the vehicle impact velocity was obtained from the PCDS report. An investigator calculated the vehicle velocity using physical evidence found at the scene (PCDS Coding and Editing Manual, 1996). The certainty of the impact velocity obtained from the PCDS reports varied from case to case and is shown in Table 1. The pedestrian's pre-impact speed was approximated by calculating the angle between the longitudinal WAD and the lateral head impact location relative to leg contact (Stammen et al., 2002). Each simulation was started at the time of initial impact. The bumper impact point on the model's leg was set as reported in the case record of damage to the vehicle. The material characteristics of the bumper for each of the simulations were approximated using a mean linear stiffness value generated from a survey of vehicle stiffness data (Stammen, 2001). The result of the first kinematic simulation was the head initial contact velocity and approach angle. This step required approximately 10 to 25 iterative simulations for each case. The simulation was then repeated again after finding the head/vehicle contact stiffness (see *Head to Hood Impact Properties* section) to obtain head accelerations for injury risk assessment.

Head to Hood Impact Properties: Experimental headform impacts were performed on seven of the vehicles using either child or adult sized pedestrian headforms conforming to International Harmonization Research Activities (IHRA) specifications, with vehicle impact data from three previous tests done by Stammen (2001) for the vehicles that were no longer available for testing. These impact tests were done at the head impact locations documented in the PCDS cases on surrogate vehicles of the same model year range as the case vehicles. The speed and angle of impact for these experimental headform tests were obtained from the initial kinematic MADYMO simulation. The headform's accelerations in the x, y, and z directions at the center of gravity were double integrated to obtain displacement and multiplied by the headform's mass to obtain force. The kinematic simulation was then conducted a second time with the experimentally determined force vs. displacement curve for the vehicle model to obtain NAAH accelerations from the MADYMO Hybrid III pedestrian model's head.

Evaluation of Simulation Accuracy: After iteratively determining the combination of pedestrian stance and vehicle speed that resulted in a consistent head impact location for simulation vs. case, a final check was made to verify that the final vehicle speed and pedestrian stance were still consistent with the case description. This check was done by examining both (a) the confidence interval for the case-documented vehicle speed in Table 1 and (b) the reported pedestrian gait type (standing, walking, jogging, or running). In addition, photographs and video of the case vehicle damage/denting attributed to head contact were compared qualitatively with the damage in the headform impact test. The sensitivity of the HIC and SIMon values to changes in the overall case reconstruction was evaluated by varying the initial contact configuration (vehicle speed, bumper-to-knee relative height) in the Dodge Ram case to get different head impact speeds and angles. The HIC and SIMon results were then evaluated with respect to those speeds and angles to confirm that the injury measures did not become unstable with respect to slight changes in head contact.

INJURY PREDICTION IN RECONSTRUCTED CASES

The x, y, and z linear accelerations measured at the center of gravity of the MADYMO head model in the simulation were used to calculate a resultant acceleration, and that acceleration was entered into the HIC algorithm and the probability of an AIS 3+ skull fracture was calculated using injury curves developed previously (Prasad, 1985, Mertz, 2003). The NAAH linear acceleration traces were input into the SIMon algorithm and the probability of brain injury was calculated.

In this study, four injury types (skull fracture, DAI, acute subdural hematoma, and brain contusion) were considered to be present only if diagnosed in the PCDS case. A documented skull fracture had to be at least AIS 3 to be considered an injury for comparison with the HIC outcome, because the HIC associated with the probability of an AIS 3+ skull fracture was used in all ten cases for consistency. Facial fractures were considered skull fractures for this analysis, with the same AIS 3+ threshold applied. For classification of DAI, ASDH, and contusion injuries, those particular injuries were identified as “injury” only if they were coded as such in PCDS.

EVALUATION OF INJURY PREDICTION MEASURES

In order to evaluate the effectiveness of the HIC, CSDM, RMDM, and DDM injury predictors in pedestrian impacts, receiver operating characteristic (ROC) classification analysis was used (Fawcett, 2006). This approach has been used extensively in the fields of signal detection and medical diagnostic testing. Using this method, the most appropriate injury probability thresholds for HIC and the three SIMon correlates in predicting the presence of a certain type of head injury in a pedestrian collision can be determined for the ten selected cases. Also, by using the area under the ROC curve (AUC), HIC and the individual SIMon correlates can be compared in their predictive accuracy (effectiveness).

ROC analysis essentially looks at the injury classifier used (for example, HIC), and allows quantification of the

quality of that classification. For example, in the data set in this study, the HIC's calculated for the reconstructed impacts ranged from 166 to 9292. Although a HIC of 166 only has a 2% chance of causing an AIS 3+ skull fracture, the possibility exists that this instance is in that 2% group. The ROC then rewards for a positive (correct) prediction and penalizes for a negative (incorrect) prediction.

ROC Curve Creation: The first step in ROC analysis is to sort the cases by decreasing "score". The term "score" in this study refers to the probability of the particular type of injury based on the injury correlate's calculated value from the simulation. For example, if a HIC value of 3133 is obtained in a simulation, the "score" would be 1.0 because HIC = 3133 corresponds to 100% probability of AIS 3+ skull fracture. Next, the binary injury designation is applied to each case. Positive, or "p", denotes a particular type of outcome or injury did occur in that case. If the case is positive, that result would be deemed a "true positive". Negative, or "n", denotes that particular outcome or injury did not occur in the case. In an ROC analysis, the best threshold value for predicting positive or negative outcomes is determined by comparing the true positive rate (TPR) and false positive rate (FPR) over the range of classifier probabilities of injury. The TPR is the total number of positives correctly classified divided by the total number of actual positive outcomes in the data set. The FPR is the total number of negatives incorrectly classified divided by the total number of actual negative (no injury) outcomes. An ROC curve plots the TPR against the FPR for each threshold considered. The ROC curve is created by incrementing in the Y direction for positive instances (injury) and X direction for negative instances (no injury).

Area Under the ROC Curve (AUC): The effectiveness of the classifier (injury correlate in this study) in predicting injury can be evaluated by calculating the area under its ROC curve, or AUC. The AUC has an important statistical property in that it is equivalent to the probability classifier will rank a randomly chosen positive instance higher than a randomly chosen negative instance (Fawcett, 2006). A diagonal line stretching from (0, 0) to (1, 1) represents the strategy of randomly guessing whether an injury occurred or not. This line corresponds to an AUC of 0.5. A larger AUC indicates that the injury correlate is a better predictor of its associated injury type. In this study, each correlate is evaluated for its effectiveness in predicting either its associated injury type or any serious head injury in a given case. The reader is referred to Hanley (1983) who gives a good discussion of the statistical basis for the AUC.

Most Accurate Threshold of ROC Curve: The most accurate threshold for predicting a positive (injury) versus negative (no injury) corresponds to the point on the ROC curve that is most toward the upper left of the graph or the furthest perpendicular distance from the diagonal line. This is the point that possesses the best combination of minimized false positive rate and maximized true positive rate. The "accuracy" associated with this point is the percentage of cases for which this threshold accurately predicts the presence or absence of the injury for those 10 cases. The injury risk associated with the most accurate point is the most appropriate threshold for the correlate in these ten cases. The quadrant in which this most accurate threshold occurs indicates whether the correlate is better at maximizing true positives or minimizing false positives. Thresholds in the upper left quadrant are the most accurate because they maximize true positives and minimize false positives. If a correlate's most accurate threshold occurs in the lower left portion of the plot, it is said to perform better in the more "conservative" region of the plot because it minimizes false positives at the expense of its ability to classify true positives. Conversely, if a correlate's most accurate threshold occurs in the upper right or more "liberal" region of the plot, it reflects that the threshold maximizes true positives but is vulnerable to false positives.

RESULTS

The pedestrian stance/speed and vehicle speed were adjusted within the constraints of documented case information (vehicle speed range, bumper impact point, pedestrian stance, preimpact pedestrian motion, head impact point) in an iterative manner in the MADYMO simulations. This was done to match of the simulated head impact location with the head impact location documented in the PCDS case. The final simulated head impact locations were consistent with the ten case-documented head impact locations longitudinally (WAD difference was 8.7 ± 4.9 cm) and laterally (2.1 ± 1.7 cm). The resultant distance (linear distance directly from the case head impact location to the simulated head impact location) was 9.0 ± 4.7 cm. Therefore, the difference between case and simulation impact points was within the 16.5 cm diameter of the headform.

An example of the MADYMO simulation and the corresponding hood damage obtained in the component test is given in Figure 2 for case 2. The simulation shows first contact of the bumper with the pedestrian's leg in the first graphic and the first head contact with the vehicle in the second graphic. The simulated pedestrian rotated 90 degrees and the occipital skull contacted the vehicle, consistent with the recorded injury in the PCDS data for this case. Table 2 summarizes the results from the second set of simulations and the probability of the pedestrian receiving the four injury modes as calculated by SIMon. For cases 9 and 10, the same experimental impact stiffness was used in each simulation since the case impacts occurred on the windshield at a similar distance away from the windshield frame. The distance between the impact and cowl in case 9 was similar to the distance between the impact and roof header in case 10. Further detail on the simulations and test results can be found in Ott (2005).

Figures 3 through 6 show the sorted data, ROC curves, and AUC for each of the four head injury correlates in the ten reconstructed cases. For each correlate, the cases were sorted by decreasing probability calculated from the simulation.

Each case was assigned a "p" if that particular injury occurred in the case and an "n" if the injury didn't occur. Using the sorted probability order, the curve is constructed by incrementally moving up if injury occurred and to the right if injury did not occur. The values in the "FP" and "TP" columns show the cumulative proportions of the total number of FP or TP for that injury type in the ten cases. For example, three of the ten cases had reported AIS 3+ skull fracture. Therefore, for each true positive (TP), the cumulative TP incrementally increased by 0.33 (1/3). Likewise, for each case without injury, the cumulative FP incrementally increased by 0.143 (1/7). The two ROC curves in each plot are for prediction of the correlate's associated injury type and ANY serious (AIS 3+) head injury present in a given case.

As shown in Figures 3, 4, 5, 6, HIC was found to be very effective at predicting AIS 3+ skull fracture in this set of ten cases with a large area under the ROC curve (AUC = 0.91). CSDM was also very effective at predicting DAI (AUC = 0.89). DDM was relatively effective (AUC = 0.68) at predicting contusion, and RMDM was only slightly more effective than random assignment of ASDH versus no ASDH (AUC = 0.56). When used to predict any AIS 3+ head injury, DDM (AUC=0.86) and RMDM (AUC=0.86) were very effective while HIC (AUC=0.67) and CSDM (AUC=0.62) were less effective.

For DDM (contusion only), the most upper left point occurred at (0.2, 0.8), while for DDM (any head injury) the most upper left point occurred at (0, 0.714). In both cases, these points corresponded to an injury risk threshold of 48%. At this 48% threshold, DDM (contusion only) was correct in 8 of 10 cases in designating the case as injury (risk >= 48%) or no injury (risk < 48%); therefore, the accuracy at this 48% threshold was 80%. Likewise, DDM (any head injury) was correct 80% of the time in these ten cases when the threshold was 48%. They both occurred in the top left region of the graph indicating maximized true positives and minimized false positives. Four of the ten potential thresholds on the DDM (contusion only) curve performed as badly as (fell on the diagonal) or worse than (fell below diagonal) randomly guessing positive versus negative. For DDM (any head injury), only one threshold was as bad as random, and that threshold was at the point that is always equal to random (1,1) because it always falls on the diagonal.

For RMDM (ASDH only), the most upper left point occurred at (0.625, 1) corresponding to an injury risk threshold of 99% at which the correlate would display 50% accuracy. This threshold is located in the most liberal region (top right) of the graph reflecting its tendency for false positives. Five of the ten thresholds were as bad as or worse than random guessing. For RMDM (any head injury), the most upper left point occurred at (0, 0.714) corresponding to an injury risk threshold of 100% (80% accuracy), and this threshold is located in the upper left region of the graph. Like DDM (any head injury), only the (1,1) point was as bad as random.

For CSDM (DAI only), the most northwest point occurred at (0.125, 1) corresponding to an injury risk threshold of 92% (90% accuracy), and this point is located in the top left region of the graph. Two of the ten thresholds were as bad as or worse than random. For CSDM (any head injury), the most upper left point occurred at (0, 0.429) corresponding to an injury risk threshold of 86% (60% accuracy), and this point is located in the most conservative region (lower left) of the graph. Three of the ten thresholds were as bad as or worse than random.

For HIC (skull fracture only), the most upper left point occurred at (0.286, 1) corresponding to an injury risk threshold of 55% (80% accuracy), and this point is located in the top left region of the graph. Only one threshold was as bad as random, and that was the point that is always equal to random (1,1). For HIC (any head injury), the most northwest point occurred at (0, 0.429) corresponding to an injury risk threshold of 79% (60% accuracy), and this point is located in the most conservative region (lower left) of the graph. Two of the ten thresholds were as bad as or worse than random.

DISCUSSION

CASE RECONSTRUCTIONS

The Hybrid III dummy is a frontal dummy and requires additional validation for use in lateral impact. The Hybrid III was used in this study due to the availability of a MADYMO model of the dummy in multiple sizes, specifically the 50th male, 5th female, and 6 year old. Use of the Hybrid III in pedestrian impact requires that the relevant kinematics of the model be validated for the pedestrian case.

Pedestrian models have been previously validated by comparing their head impact velocities in pedestrian impacts with post-mortem human subjects for a consistent speed and vehicle geometry (Stammen (2001), Ishikawa et al. (1993)). The time history for head resultant velocity of the Hybrid III model relative to post-mortem human subject (PMHS) corridors for the same vehicle geometry at 32 km/h are given in Figure 7. The Hybrid III model used in this validation simulation was scaled to match the height and weight of the average PMHS per Ishikawa et al. (1993). The results given in Figure 7 indicate that the Hybrid III model's head velocity provides a reasonable approximation of the PMHS velocities.

In addition, the simulations resulted in similar head impact locations as recorded in the case records while maintaining the documented pedestrian and vehicle characteristics. The distance between the case impact location and the simulated impact location was less than the diameter of the simulated head itself in nine out of the ten reconstructions. The vehicle damage from the case versus the experimental headform impact was also consistent for the ten cases by qualitative comparison of PCDS photographs and the damage to the vehicle in the impact tests.

INJURY CONSIDERATIONS

In this study, skull and facial fractures in cases 1 and 9 were not considered injuries because they were not AIS 3 or greater. For consistency, the HIC resulting from the simulation was correlated with the probability of AIS 3+ skull/facial fracture for all ten cases. The HIC calculated in the simulation for case 3 of 2338 is consistent with the reported impact speed of the striking vehicle of 48kph. However, the 8 year old child subject in this case received only minor head injuries below AIS 3 (bilateral cheek contusions, abrasion to the lip, 3 minute loss of consciousness with amnesia). The simulations of cases 1 and 3 calculated high HIC (3133 and 2338 respectively) but neither of the accident subjects in these cases sustained an AIS 3+ head injury. It may be relevant to note that both of these accident subjects were children (ages 6 and 8 respectively) and their age may have been a factor in their minimal injury. This observation indicates a need for a greater sample size. The fact that the simulations of the children pedestrians did not produce injury indicators consistent with the recorded injuries indicates a need to separate children from adults in further study.

While cases 1, 7, and 8 had symptoms that are consistent with the presence of DAI, including loss of consciousness for greater than 6 hours, other injuries documented in those cases could have resulted in the same symptoms. Case 1 was listed with intraventricular hemorrhage/intracerebral hematoma in the ventricular system, uncal and cerebellar herniation, diffuse edema, and subarachnoid hemorrhage. Case 7 was listed with subdural hematoma, brain stem injury (possibly shear), subarachnoid hemorrhage, and bilateral temporal contusions. Case 8 had a large epidural hematoma around the cord, subarachnoid hemorrhage at the brain stem, brain stem injury, and mid-brain swelling with edema. According to the AIS 90 convention for coding DAI in the PCDS, the diagnosis of the DAI injury is made by a combination of clinical observations, i.e. immediate and prolonged coma lasting more than 6 hours, and CT and or magnetic resonance imaging brain images that do not demonstrate prolonged hypotension or infarction, mass lesion (epidural, subdural, or intracerebral hematoma) that explain the coma. This definition has also been used in other case data studies of head injuries (Yoganandan et al, 2009). Of the three cases that were not coded with a DAI AIS code but were listed with greater than 6 hours of unconsciousness, none of the three meet the criteria suggested by the AIS 90 criteria and therefore are coded based on available injury information.

ROC ANALYSIS

ROC analysis is an established and quantitative approach to examine effectiveness of various injury correlates in the prediction of injury. The area under the ROC curve (AUC) is statistically equivalent to the probability that the correlate will rank a randomly chosen positive instance (injury) higher than a randomly chosen negative instance (no injury). Therefore, a higher AUC value corresponds to better overall effectiveness. Examination of the overall shape of the ROC curve gives information on how the correlate performs in different areas of the plot. For example, when a large portion of the ROC curve's AUC is in the lower left corner, it indicates that the correlate performs better in the low true/low false positive range. Conversely, a larger portion of AUC in the upper right corner indicates better performance in the range of high true/high false positive rate. The upper left-most point on the ROC curve corresponds to the appropriate injury risk threshold for distinguishing between injury and no injury. The associated accuracy for that specific, upper left-most threshold level is the percentage of cases for which the presence or absence of the injury was accurately predicted using that most appropriate injury risk threshold. If the data set analyzed is representative of the entire population of all possible observations, then inclusion of additional cases simply reduces the size of the steps in the ROC curve without changing its general shape. As the data set approaches infinity, the ROC curve smoothes, again maintaining its general shape. The ROC curve is very sensitive to outliers in that a penalty is levied against cases where the probability of being either positive or negative is large but the case is incorrectly predicted (i.e., no injury with a HIC of 3133). In situations where the data set is small, such penalties have a large influence on the shape of the curve and the AUC. When the results shown in Table 3 are taken together, AUC provides an assessment of that correlate's overall performance while accuracy illustrates how well the correlate performs for these ten cases only. Because it is less sensitive to individual cases, AUC is the primary element in evaluating the correlates in this study.

RMDM was only slightly more effective than random assignment of an injury versus no injury (AUC = 0.56). A possible explanation for RMDM being the least effective predictor of its corresponding injury is that this correlate was only based on sagittal impact data (Takhounts, 2003). Five of the ten simulation cases (cases 1, 4, 6, 9 and 10) involved impacts that were not purely in the sagittal plane.

Figures 9 through 12 show the results of Consistent Threshold Analysis, another nonparametric statistical technique that can be used to analyze this data. These curves are presented here only for reference, as the ROC curves provide sufficient basis for the conclusions presented here. The interested reader can study and compare the ROC and CT as desired.

SENSITIVITY OF INJURY CORRELATES TO RECONSTRUCTION PARAMETERS

To assess the sensitivity of the injury results to changes in the head contact velocity, approach angle, and inverse tangent of tangential/normal force (Figure 8), the Dodge Ram case initial conditions were adjusted. These adjustments included vehicle impact speed and the relative bumper-to-knee height

for the initial contact. The vehicle profile, vehicle stiffness (regardless of changes in WAD), and pedestrian model remained constant throughout. Table 4 summarizes the results.

The choice of the Dodge Ram case for the sensitivity study was based on the assumption that it would produce more variation in head response than a case involving a lower profile hood. This assumption proved to be correct as is evidenced by the wide variation in head approach angle. This variation in head angle is due to the sensitivity of the shoulder's interaction with the hood leading edge. A smaller vehicle would be expected to have less sensitivity of injury correlates to vehicle speed/bumper-to-knee height.

A statistical analysis was done to examine sensitivity of the injury correlates to the head contact conditions from the reconstruction. A multiple regression analysis was done on each of the four injury correlates to determine the sensitivity of each correlate to head contact velocity and angle (Table 5). All four of the injury correlates had an R-squared value above 0.9. For HIC and RMDM, all three of the head input conditions had a significant effect ($p<0.05$). For CSDM, head velocity and angle were significant, while theta did not meet a statistical significance of $p<0.05$. For DDM, both angles were significant while velocity was not. This statistical analysis indicates that each of the injury correlates are predictably related to the head input conditions. The model is thus stable and follows the real-world observation that injury becomes more severe when the head contact occurs at a higher speed and a more perpendicular angle to the hood. The only negative correlation was DDM with angle, which is expected due to the head rotating about the shoulder more when the approach angle is lower (more horizontal hood).

The reconstruction process in this study consisted of matching the case head impact location by adjusting the initial conditions (vehicle speed, bumper-to-knee height) within the uncertainty bounds of the case documentation. For each of the ten cases, the head model came within one head diameter of the case head impact location. This consistency required much smaller variations in vehicle speed and bumper-to-knee height than those shown in Table 4. For the Dodge Ram case specifically, the uncertainty bound for the vehicle speed was 23 - 25 km/hr and the bumper-to-knee contact was limited within the breadth of the bumper (+ 2 cm to - 1 cm from the reported contact). Using these ranges, the expected head input conditions for the Dodge Ram would be within a small range. Therefore, the actual error bars for vehicle speed/bumper-to-knee height in the case, through small variation in head input conditions, would result in a reduced range of injury correlate values than what is presented in this sensitivity analysis.

Because (a) the injury correlates were found to have predictable and realistic relationships with head input conditions for this case and (b) the iteration range for a given case is a small portion of the sensitivity range investigated here, it is concluded that the relative effectiveness of injury measures for the full dataset of 10 cases would not change significantly from what is reported. Although the sensitivity of the injury correlates to variations in head input conditions for the other vehicle cases was not studied, the importance of the interaction between the shoulder and the hood leading edge for the Dodge Ram case would result in greater sensitivity than smaller vehicles to the relationship between injury correlates and initial vehicle speed/bumper-to-knee height. The indication is that the injury correlates are predictably related to small perturbations of impact conditions.

COMBINED PEDESTRIAN HEAD INJURY ASSESSMENT STRATEGY

If HIC is to be used alone to predict pedestrian head injury, HIC must not only be accurate in predicting skull fracture but also be accurate in predicting brain injuries. While it was shown that HIC is very effective at predicting AIS 3+ skull fracture, it was much less effective at predicting *any* serious head injury. Because pedestrians often experience a combination of loading modes, HIC may be limited because it accounts for linear acceleration only. Although linear acceleration is often correlated with other loading modes, it may not be enough to capture the complexity and variability of pedestrian head impacts. Correlates that capture those other loading modes, such as those in SIMon, may supplement the risk measured by HIC. SIMon has correlates that seem to be very effective at predicting any head injury. For example, the fact that DDM and RMDM are more effective than HIC at predicting any AIS 3+ head injury suggests that they capture high-risk loading that may not be captured by HIC. In addition, CSDM was very effective at predicting DAI, which has been shown to be associated with rotational loading. By supplementing HIC with correlates that capture other loading patterns present in pedestrian cases, head injury risk would be more robustly evaluated. While there were not enough cases in this study to evaluate specific combinations of HIC with SIMon correlates or make any definite conclusions using ROC analysis, the results do suggest benefits of a combined head injury assessment strategy.

CONCLUSIONS

- In a PCDS analysis, the majority of pedestrians sustained head injuries from a combination of both rotational and translational mechanisms.

- Using the area under curve (AUC) value, HIC (AUC=0.91) and CSDM (AUC=0.89) were very effective at predicting skull fracture and DAI, respectively. DDM (AUC=0.68) and RMDM (AUC=0.56) were less effective at predicting their associated injury types (contusion and acute subdural hematoma, respectively).

- When the injury correlates were each evaluated against any AIS 3+ head injury instead of the associated injury type only, DDM and RMDM (both AUC=0.86) performed better than

they did in predicting only their associated injury. Conversely, HIC (AUC=0.67) and CSDM (AUC=0.62) were less effective in predicting any AIS 3+ head injury.

• The injury measures were found to be quite sensitive to the initial pedestrian-vehicle contact (bumper-to-knee height, vehicle speed, etc.) because of cumulative errors in developing the head-to-vehicle contact condition. While care was taken to match the head contact conditions between case and simulation, it cannot be quantified whether the simulation head contact perfectly represented the head-to-vehicle interaction from the case.

• For the ten cases evaluated in this study, each correlate was strong at predicting either its associated injury or any head injury. However, there was no single injury correlate that performed effectively in predicting both its associated injury and any AIS 3+ head injury. Because pedestrian head injuries are often associated with a combination of linear and rotational loading, supplementing HIC with correlates that capture other loading patterns could lead to more robust head injury assessment.

REFERENCES

1. Abel, J., Gennarelli, T., and Segawa, H., "Incidence and Severity of Cerebral Concussion in the Rhesus Monkey Following Sagittal Plane Angular Acceleration," SAE Technical Paper 780886, 1978, doi: 10.4271/780886.
2. Alexander, M.P. (1995) Mild Traumatic Brain Injury: Pathophysiology, Natural History, and Clinical Management. *Neurology*, Vol 45(7), pp. 1253-60.
3. Arbogast, K.B. Jermakian, J.S., Ghati, Y. Smith, R. Maltese, M.R., Menon, R.A. (2005) Predictors and Patterns of Pediatric Head Injury in Motor Vehicle Crashes. *IRCOBI*, 2005, pp. 15-28.
4. Chidester, AB, Isenberg, RA. (2001) Final report-the pedestrian crash data study. *Proceedings of the 17th International Conference on the Enhanced Safety of Vehicles (ESV)*; Paper No 248.
5. DiMasi, F.P. (1995) Transformation of Nine-Accelerometer-Package (NAP) Data for Replicating Headpart Kinematics and Dynamic Loading. *NHTSA Report #* DOT-HS-808-282.
6. Fawcett, T. (2006) An Introduction to ROC Analysis. Pattern Recognition Letters Vol 27(2006) pp. 861-874.
7. Gennarelli, T.A., et al. (1982) Diffuse Axonal Injury and Traumatic Coma in the Primate. Ann Neurol 12: 564-574.
8. Gennarelli, T.A. (1993) Mechanisms of Brain Injury. *J. Emergency Medicine*, Suppl 1, pp. 5-11.
9. Gentleman, S.M., Roberts, G.W., Gennarelli, T.A., Maxwell, W.L., Adams, J.H., Kerr, S. Graham, D.I. (1995) Axonal Injury: A Universal Consequence of Fatal Closed Head Injury? *Acta Neuropathologica*, Vol 89(6), pp. 537-43.
10. Hanley, J.A., McNiel, B.J., "The Meaning and Use of the Area Under The Receiver Operating Characteristic (ROC) Curve", *Radiology* 1982 143 29-36.
11. Hardy, W., Foster, C., Mason, M., Yang, K. et al., "Investigation of Head Injury Mechanisms Using Neutral Density Technology and High-Speed Biplanar X-ray," SAE Technical Paper 2001-22-0016, 2001.
12. Ishikawa, H., Kajzer, J., and Schroeder, G., "Computer Simulation of Impact Response of the Human Body in Car- Pedestrian Accidents," SAE Technical Paper 933129, 1993, doi: 10.4271/933129.
13. IHRA. (2001) International Harmonized Research Activities Pedestrian Safety Working Group 2001 Report. *IHRA/PA/2001*.
14. Kallieris, D., Rizzetti, A., Mattern, R. (1997) Some Observations to the Skull-Brain Trauma. *Advisory Group for Aerospace Research and Development Conference 597*, pp. 1-4.
15. Kamalakkannan, S., Guenther, D., Wiechel, J., and Stammen, J., "MADYMO Modeling of the IHRA Head-form Impactor," SAE Technical Paper 2005-01-2740, 2005, doi:10.4271/2005-01-2740.
16. Levi, L. Guilburd, J.N., Lemberger, A., Soustiel, J.F., Feinsod, M. (1990) Diffuse Axonal Injury: Analysis of 100 Patients with Radiological Signs. *Neurosurgery*, Vol. 27(3), pp. 429-32.
17. Lissner, H., Lebow, M. and Evans, F. (1960) Experimental Studies on the Relation Between Acceleration and Intracranial Changes in Man. *Surgery, Gynecology & Obstetrics*, Vol. 11. pp. 329-38.
18. Meaney, D.F., Smith, D., Ross, D.T., Gennarelli, T.A. (1993) Diffuse axonal injury in the miniature pig: Biomechanical development and injury threshold. *ASME Crashworthiness and occupant protection systems*, Vol. 25, 169-75.
19. Mertz, H., Irwin, A., and Prasad, P., "Biomechanical and Scaling Bases for Frontal and Side Impact Injury Assessment Reference Values," SAE Technical Paper 2003-22-0009, 2003.
20. NHTSA, NCSA. (2009) Traffic Safety Facts, 2008, Traffic Safety Annual Assessment. DOT HS 811 172.
21. Nusholtz, G.S., Wylie, B. Glascoe, L.G. (1995) Cavitation/Boundary effects in a simple head impact model. *Aviation Space & Environmental Medicine*, Vol. 66(7), 661-667.
22. Ott, K. (2005) Traumatic Brain Injury (TBI) in Pedestrian Collisions. Master's Thesis, The Ohio State University.
23. Prasad, P. and Mertz, H., "The Position of the United States Delegation to the ISO Working Group 6 on the Use of HIC in the Automotive Environment," SAE Technical Paper 851246, 1985, doi: 10.4271/851246.
24. Sahuguillo-Barris, J., Lamarca-Ciuro, J., Vilalta-Castan, J., Rubio-Garcia, E., Rodriguez-Pazos, M. (1988) Acute Subdural Hematoma and Diffuse Axonal Injury after Severe Head Trauma. *J. Neurosurgery*, Vol. 68(6), 894-900.
25. Stalnaker, R.L., Alem, N.M., Benson, J.B., Melvin, J.W. (1977) Validation studies for head impact injury model. Final report DOT HS-802 566.
26. Stammen, J., Barsan-Anelli, A. (2001) Adaptation of a Human Body Mathematical Model to Simulation of Pedestrian/Vehicle Interactions. *4th MADYMO User's Meeting of The America's*.
27. Stammen, J., Ko, S., Guenther, D., and Heydinger, G., "A Demographic Analysis and Reconstruction of Selected Cases from the Pedestrian Crash Data Study," SAE Technical Paper 2002-01-0560, 2002, doi: 10.4271/2002-01-0560.
28. Takhounts, E., Eppinger, R., Campbell, J., Tannous, R. et al., "On the Development of the SIMon Finite Element Head Model," SAE Technical Paper 2003-22-0007, 2003.
29. U.S. Department of Transportation, NCSA. (1996) 1996 Pedestrian Crash Data Study, Data Collection, Coding, and Editing Manual. US DOT, NCSA, October.
30. Versace, J., "A Review of the Severity Index," SAE Technical Paper 710881, 1971, doi: 10.4271/710881.
31. Vorst, M.V., Stuhmiller, J., Ho, K., Yoganandan, N., Pintar, F. (2003) Statistically and Biomechanically Based Criterion for Impact-Induced Skull Fracture. *Annu Proc Assoc Adv Automot Med.* 47, pp. 363-81.
32. Yoganandan, N, Gennarelli, TA, Zhang, J, Pintar, FA, Takhounts, E, Ridella, S, "Association of Contact Loading in Diffuse Axonal Injuries from Motor Vehicle Crashes," Journal of Trauma, 66:309-315, 2009.
33. Yoshida, S., Igarashi, N., Takahashi, A., and Imaizumi, I., "Development of a Vehicle Structure with Protective Features for Pedestrians," SAE Technical Paper 1999-01-0075, 1999, doi: 10.4271/1999-01-0075.

CONTACT INFORMATION

Contact Author:
John Wiechel
The Ohio State University
7349 Worthington-Galena Road
Columbus, Ohio 43085
614-888-4160
wiechel.4@osu.edu

ACKNOWLEDGMENTS

Special thanks to David Hyder for help with the experimental headform testing and Aida Barsan-Anelli for conducting the parameter sensitivity study. This work was funded under NHTSA contract. Any opinions or conclusions made in this paper based on the data are those of the co-authors and are not necessarily those of their respective organizations.

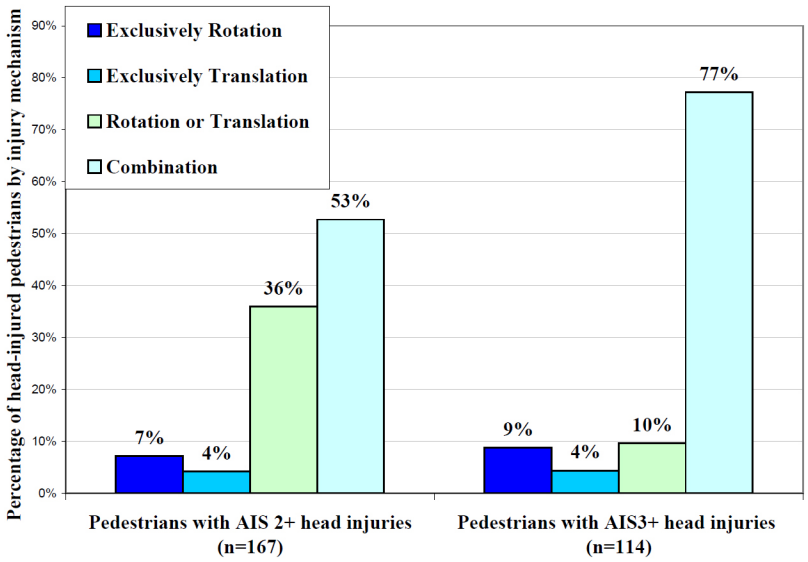

Figure 1. Head-Injured Pedestrians in PCDS Classified by Injury Mechanism

Table 1. Reconstructed PCDS cases.

Case #	PCDS Case	Vehicle Model/Year	Age	Sex	Height (cm)	Weight (kg)	MAIS (Head)	Vehicle Impact Speed (km/h)	Vehicle Impact Speed Confidence Interval (km/h)
1	96-72-619P	1994 Plymouth Sundance	6	M	102	20	5	30	2 - 8
2	96-82-646P	1996 Dodge Ram	47	M	165	57	4	24	≤ 2
3	97-49-603P	1989 Toyota Celica	8	F	138	62	2	40	2 - 8
4	96-90-601P	1992 Plymouth Voyager	55	M	182	83	1	28	9 - 16
5	96-41-602P	1994 Ford F150	42	M	168	50	5	32	≤ 2
6	98-82-608P	1996 Ford Taurus	48	M	178	82	2	27	≤ 2
7	96-49-625P	1993 Honda Civic	13	M	152	43	5	38	≤ 2
8	97-90-618P	1996 Chevrolet Cavalier	33	F	170	60	5	67	≤ 2
9	97-82-644P	1990 Honda Civic	25	F	150	57	3	32	≤ 2
10	96-82-629P	1990 Honda Civic	47	M	196	98	3	31	≤ 2

Table 2. Simulation Results and Associated Injuries from Ten PCDS Case Reconstructions

Case	Injury Type	Injury	Injury Correlate Value from Simulation	Injury Probability
1	Contusion	None	DDM = 0.027	23%
	ASDH	None	RMDM = 4.81	100%
	DAI	None	CSDM = 0.650	65%
	AIS 3+ Skull Fx	None (Temporal Fx but AIS 2)	HIC = 3133	79%
	Other AIS 3+	Multiple hemorrhages (AIS 3 right subarachnoid, AIS 4 intraventricular, AIS 4 intracerebral), AIS 5 brain stem compression, AIS 5 loss of consciousness 6 – 24 hrs with neurological deficit		
2	Contusion	Small Frontal Contusion (AIS 3)	DDM = 0.069	48%
	ASDH	Frontal-Parietal SDH (AIS 4)	RMDM = 2.21	99%
	DAI	None	CSDM = 0.432	33%
	AIS 3+ Skull Fx	None	HIC = 275	0.7%
	Other AIS 3+	None		
3	Contusion	None	DDM = 0.003	10%
	ASDH	None	RMDM = 0.844	40%
	DAI	None	CSDM = 0.602	60%
	AIS 3+ Skull Fx	None	HIC = 2338	66%
	Other AIS 3+	None		
4	Contusion	None	DDM = 0.032	25%
	ASDH	None	RMDM = 2.24	99%
	DAI	None	CSDM = 0.664	70%
	AIS 3+ Skull Fx	None	HIC = 740	12.7%
	Other AIS 3+	None		
5	Contusion	Large Parietal Contusion (AIS 4)	DDM = 0.084	60%
	ASDH	None	RMDM = 4.13	100%
	DAI	Cerebrum DAI/Shearing (AIS 5)	CSDM = 0.925	93%
	AIS 3+ Skull Fx	Basilar Skull Fx (AIS 3)	HIC = 1904	55.3%
	Other AIS 3+	Left & right cerebrum edema (AIS 3)		
6	Contusion	None	DDM = 0.015	15%

Table 2 (cont.). Simulation Results and Associated Injuries from Ten PCDS Case Reconstructions

	ASDH	None	RMDM = 1.76	96%
	DAI	None	CSDM = 0.148	15%
	AIS 3+ Skull Fx	None	HIC = 166	0.1%
	Other AIS 3+	None		
7	Contusion	Temporal Contusions (AIS 3)	DDM = 0.124	82%
	ASDH	Right SDH (AIS 4)	RMDM = 6.53	100%
	DAI	None	CSDM = 0.860	86%
	AIS 3+ Skull Fx	Multiple Fx (AIS 3)	HIC = 6868	96.9%
	Other AIS 3+	AIS 3 edema, AIS 3 subarachnoid hemorrhage, AIS 5 loss of consciousness > 24 hrs		
8	Contusion	None	DDM = 0.315	100%
	ASDH	None	RMDM = 8.17	100%
	DAI	None	CSDM = 0.925	93%
	AIS 3+ Skull Fx	L/R Occipital Fx (AIS 3)	HIC = 9292	98.9%
	Other AIS 3+	AIS 5 brain stem hemorrhage, AIS 5 loss of consciousness		
9	Contusion	Temporal Contusions (AIS 3)	DDM = 0.095	69%
	ASDH	None	RMDM = 1.45	86%
	DAI	None	CSDM = 0.015	1%
	AIS 3+ Skull Fx	None (Parietal Fx but AIS 2)	HIC = 215	0.2%
	Other AIS 3+	None		
10	Contusion	Temporal Contusions (AIS 3)	DDM = 0.014	14%
	ASDH	None	RMDM = 3.16	100%
	DAI	None	CSDM = 0.301	30%
	AIS 3+ Skull Fx	None	HIC = 774	14%
	Other AIS 3+	None		

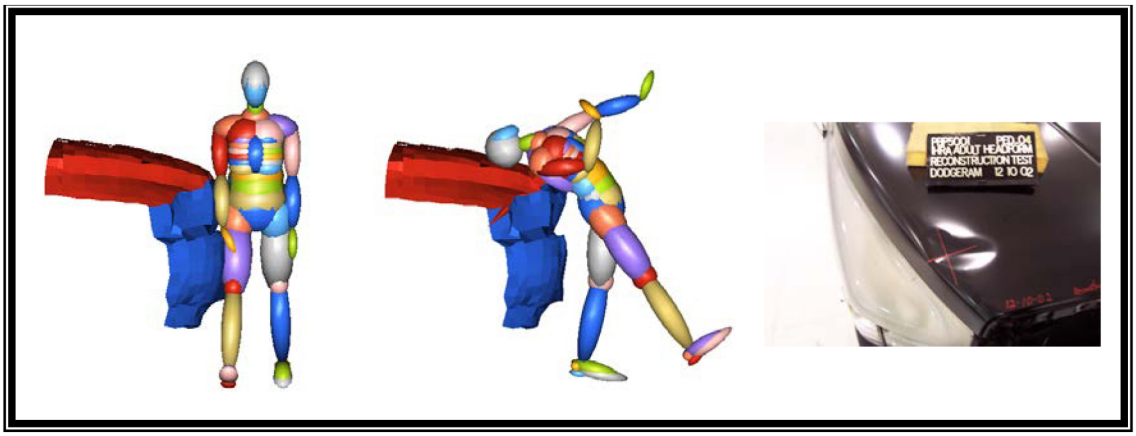

Figure 2. Case 2 MADYMO simulation at initial leg contact (left) and subsequent head contact (center). Vehicle damage from headform impact test to derive stiffness for simulation (right). This vehicle damage compared well with photographic documentation of the case vehicle (not shown).

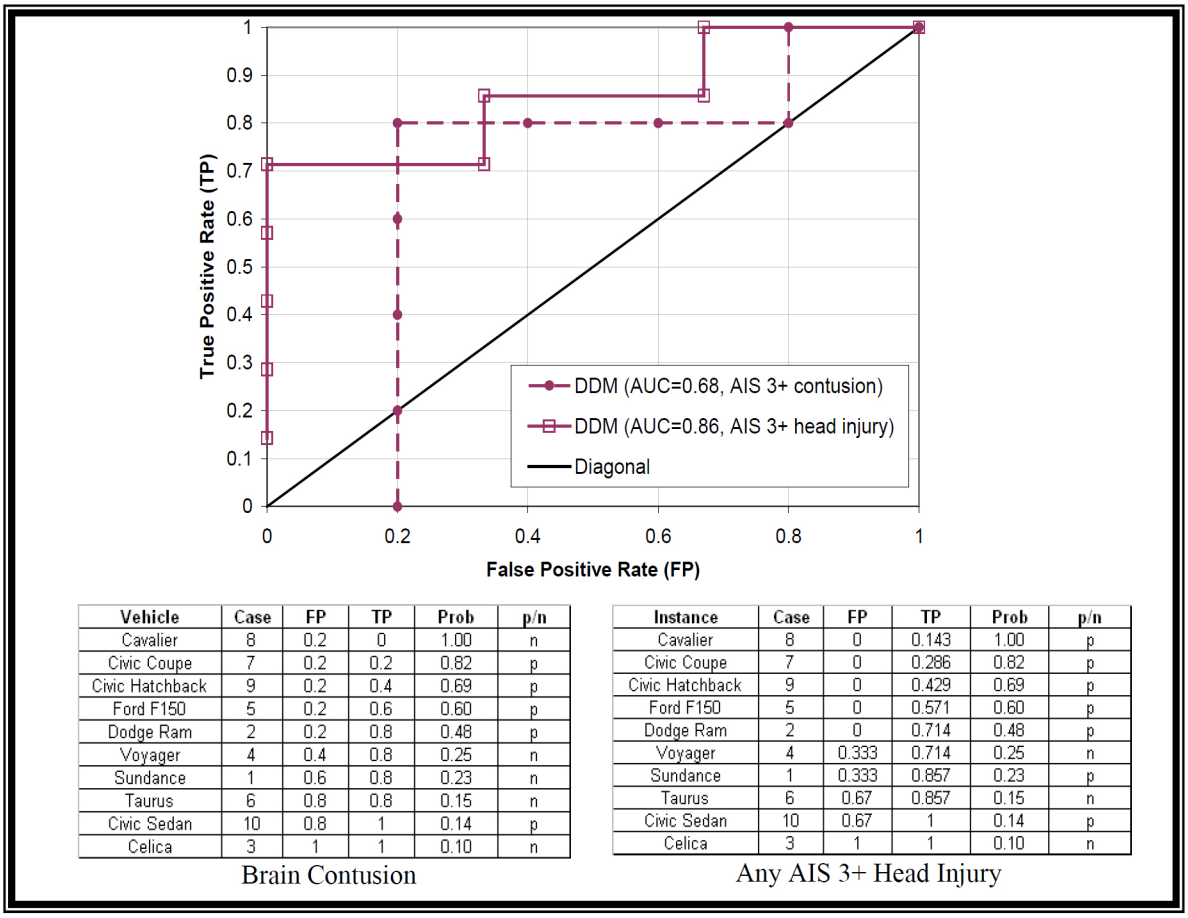

Vehicle	Case	FP	TP	Prob	p/n
Cavalier	8	0.2	0	1.00	n
Civic Coupe	7	0.2	0.2	0.82	p
Civic Hatchback	9	0.2	0.4	0.69	p
Ford F150	5	0.2	0.6	0.60	p
Dodge Ram	2	0.2	0.8	0.48	p
Voyager	4	0.4	0.8	0.25	n
Sundance	1	0.6	0.8	0.23	n
Taurus	6	0.8	0.8	0.15	n
Civic Sedan	10	0.8	1	0.14	p
Celica	3	1	1	0.10	n

Brain Contusion

Instance	Case	FP	TP	Prob	p/n
Cavalier	8	0	0.143	1.00	p
Civic Coupe	7	0	0.286	0.82	p
Civic Hatchback	9	0	0.429	0.69	p
Ford F150	5	0	0.571	0.60	p
Dodge Ram	2	0	0.714	0.48	p
Voyager	4	0.333	0.714	0.25	n
Sundance	1	0.333	0.857	0.23	p
Taurus	6	0.67	0.857	0.15	n
Civic Sedan	10	0.67	1	0.14	p
Celica	3	1	1	0.10	n

Any AIS 3+ Head Injury

Figure 3. ROC for SIMon DDM Identification of Brain Contusion or Any Head Injury. Standard error is 0.108 for AIS 3+ contusion and 0.12 for AIS 3+ head injury.

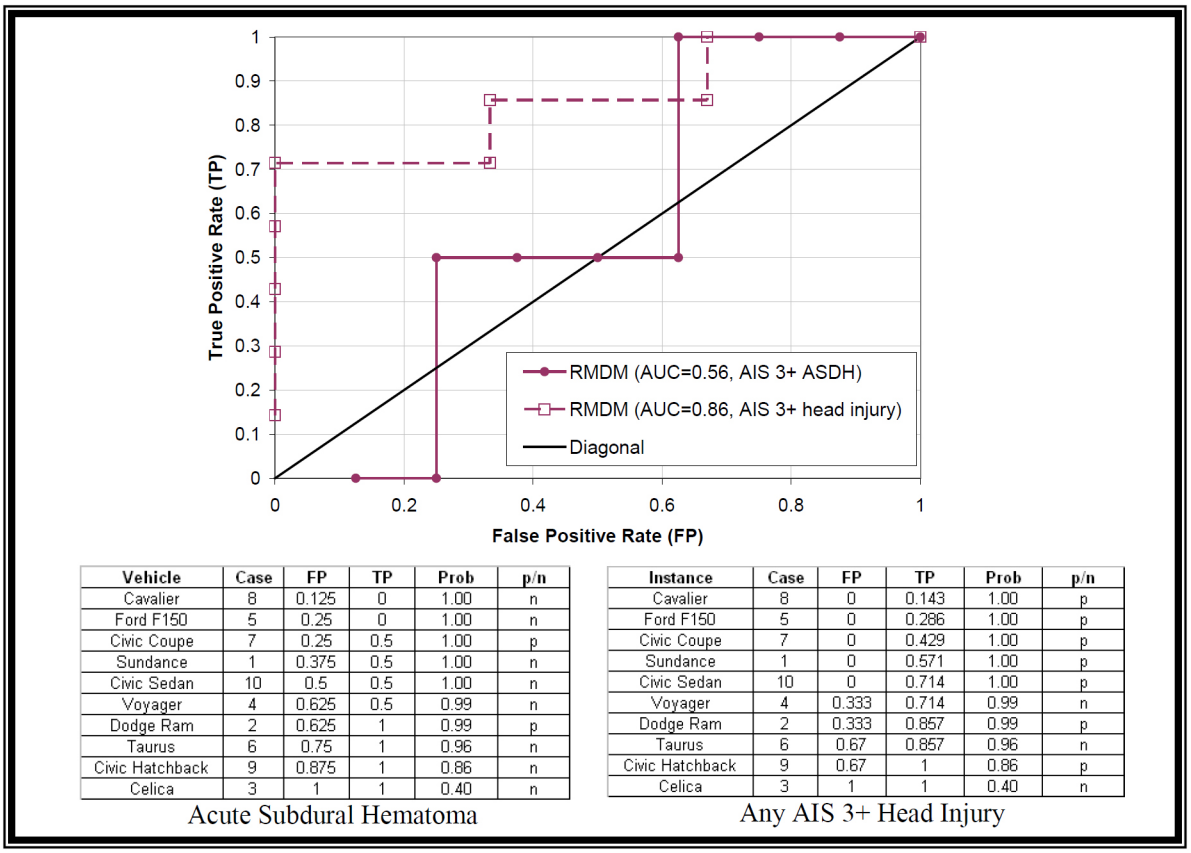

Vehicle	Case	FP	TP	Prob	p/n
Cavalier	8	0.125	0	1.00	n
Ford F150	5	0.25	0	1.00	n
Civic Coupe	7	0.25	0.5	1.00	p
Sundance	1	0.375	0.5	1.00	n
Civic Sedan	10	0.5	0.5	1.00	n
Voyager	4	0.625	0.5	0.99	n
Dodge Ram	2	0.625	1	0.99	p
Taurus	6	0.75	1	0.96	n
Civic Hatchback	9	0.875	1	0.86	n
Celica	3	1	1	0.40	n

Acute Subdural Hematoma

Instance	Case	FP	TP	Prob	p/n
Cavalier	8	0	0.143	1.00	p
Ford F150	5	0	0.286	1.00	p
Civic Coupe	7	0	0.429	1.00	p
Sundance	1	0	0.571	1.00	p
Civic Sedan	10	0	0.714	1.00	p
Voyager	4	0.333	0.714	0.99	n
Dodge Ram	2	0.333	0.857	0.99	p
Taurus	6	0.67	0.857	0.96	n
Civic Hatchback	9	0.67	1	0.86	p
Celica	3	1	1	0.40	n

Any AIS 3+ Head Injury

Figure 4. ROC for SIMon RMDM Identification of Acute Subdural Hematoma or Any Head Injury. Standard error is 0.21 for AIS 3+ASDH and 0.12 for AIS 3+ head injury.

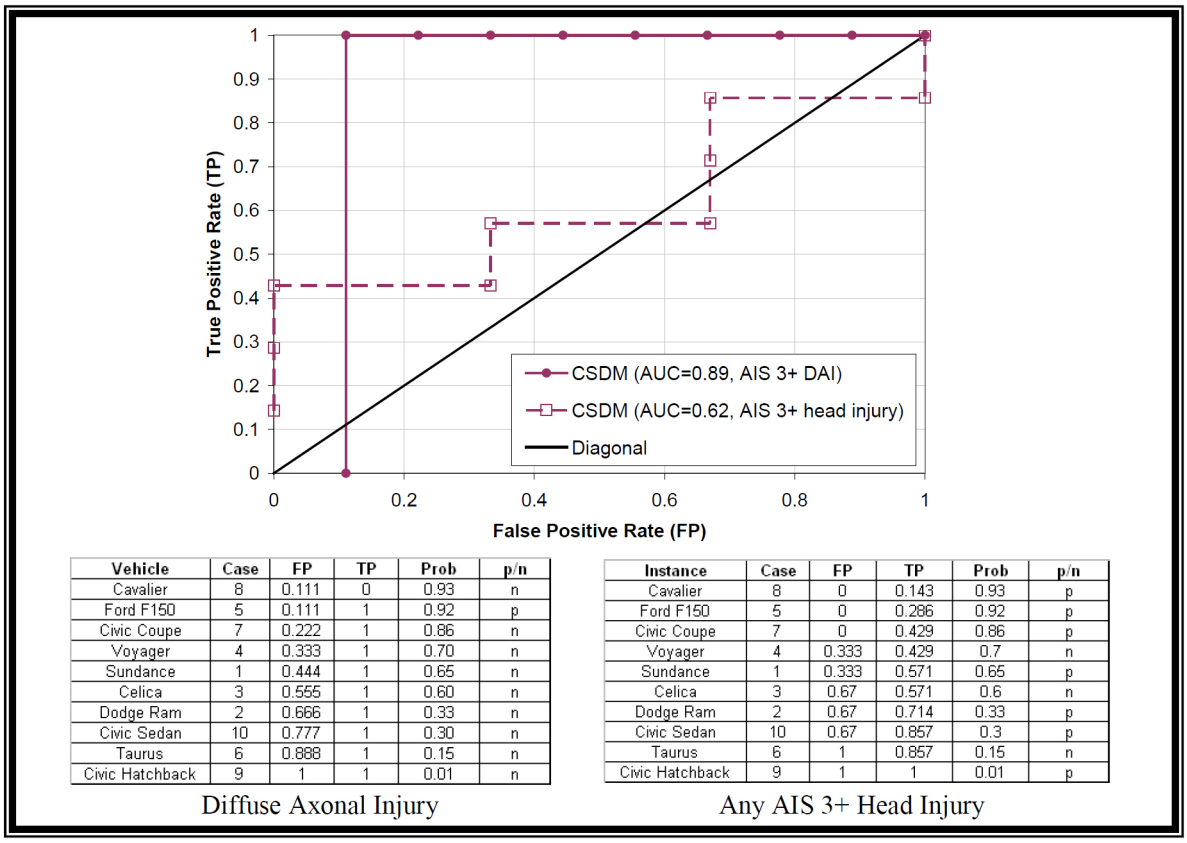

Vehicle	Case	FP	TP	Prob	p/n
Cavalier	8	0.111	0	0.93	n
Ford F150	5	0.111	1	0.92	p
Civic Coupe	7	0.222	1	0.86	n
Voyager	4	0.333	1	0.70	n
Sundance	1	0.444	1	0.65	n
Celica	3	0.555	1	0.60	n
Dodge Ram	2	0.666	1	0.33	n
Civic Sedan	10	0.777	1	0.30	n
Taurus	6	0.888	1	0.15	n
Civic Hatchback	9	1	1	0.01	n

Diffuse Axonal Injury

Instance	Case	FP	TP	Prob	p/n
Cavalier	8	0	0.143	0.93	p
Ford F150	5	0	0.286	0.92	p
Civic Coupe	7	0	0.429	0.86	p
Voyager	4	0.333	0.429	0.7	n
Sundance	1	0.333	0.571	0.65	p
Celica	3	0.67	0.571	0.6	n
Dodge Ram	2	0.67	0.714	0.33	p
Civic Sedan	10	0.67	0.857	0.3	p
Taurus	6	1	0.857	0.15	n
Civic Hatchback	9	1	1	0.01	p

Any AIS 3+ Head Injury

Figure 5. ROC for SIMon CSDM Identification of Diffuse Axonal Injury (DAI) or Any Head Injury. Standard error is 0.23 for AIS 3+ DAI and 0.20 for AIS 3+ head injury.

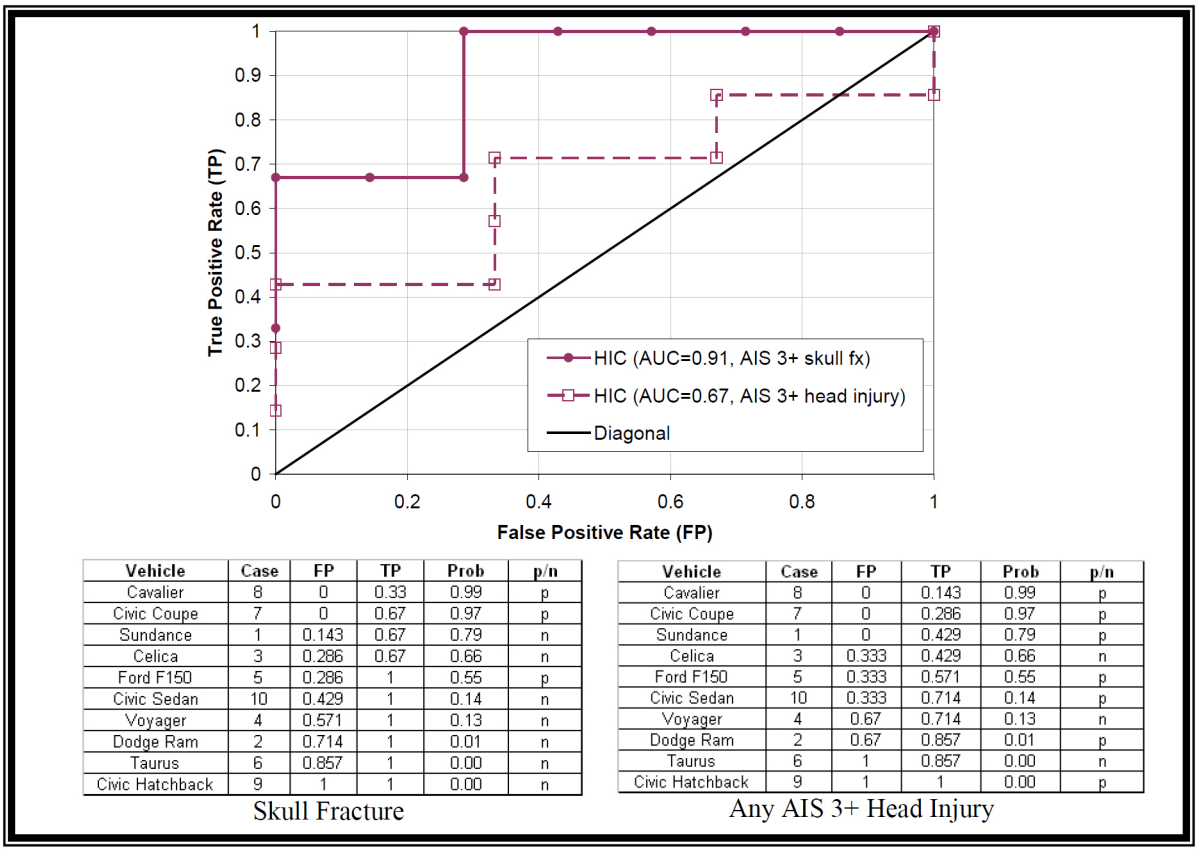

Vehicle	Case	FP	TP	Prob	p/n
Cavalier	8	0	0.33	0.99	p
Civic Coupe	7	0	0.67	0.97	p
Sundance	1	0.143	0.67	0.79	n
Celica	3	0.286	0.67	0.66	n
Ford F150	5	0.286	1	0.55	p
Civic Sedan	10	0.429	1	0.14	n
Voyager	4	0.571	1	0.13	n
Dodge Ram	2	0.714	1	0.01	n
Taurus	6	0.857	1	0.00	n
Civic Hatchback	9	1	1	0.00	n

Skull Fracture

Vehicle	Case	FP	TP	Prob	p/n
Cavalier	8	0	0.143	0.99	p
Civic Coupe	7	0	0.286	0.97	p
Sundance	1	0	0.429	0.79	p
Celica	3	0.333	0.429	0.66	n
Ford F150	5	0.333	0.571	0.55	p
Civic Sedan	10	0.333	0.714	0.14	p
Voyager	4	0.67	0.714	0.13	n
Dodge Ram	2	0.67	0.857	0.01	p
Taurus	6	1	0.857	0.00	n
Civic Hatchback	9	1	1	0.00	p

Any AIS 3+ Head Injury

Figure 6. ROC for HIC Identification of Skull Fracture or Any Head Injury. Standard error is 0.13 for AIS 3+ skull fx and 0.109 for AIS 3+ head injury.

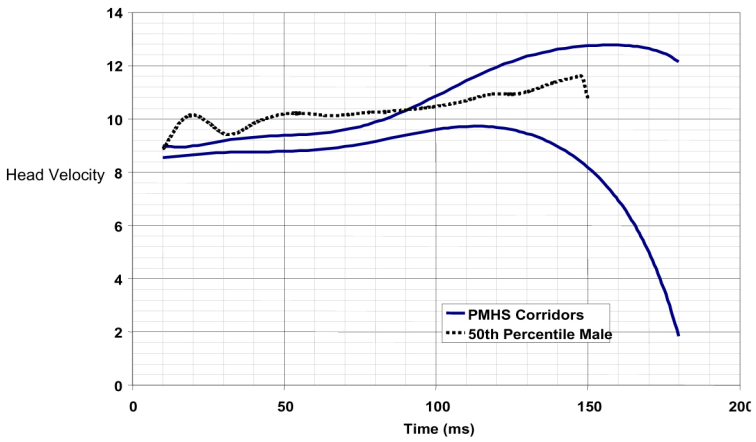

Figure 7. Head Resultant Velocity (PMHS Corridors from Ishikawa, 1993)

Table 3. Summary of ROC Results for Each Injury Correlate

	Global Correlate Assessment	Correlate Assessment for These 10 Cases Only		
Injury Correlate	Area Under ROC Curve (AUC)	Quadrant of Most Northwest Point	Most Accurate Injury Risk Threshold	Accuracy for Most Accurate Injury Risk Threshold
DDM (Contusion)	0.68	Top Left	48%	80%
DDM (Any Head Injury)	0.86	Top Left	48%	80%
RMDM (ASDH)	0.56	Top Right	99%	50%
RMDM (Any Head Injury)	0.86	Top Left	100%	80%
CSDM (DAI)	0.89	Top Left	92%	90%
CSDM (Any Head Injury)	0.62	Bottom Left	86%	60%
HIC (Skull Fracture)	0.91	Top Left	55%	80%
HIC (Any Head Injury)	0.67	Bottom Left	79%	60%

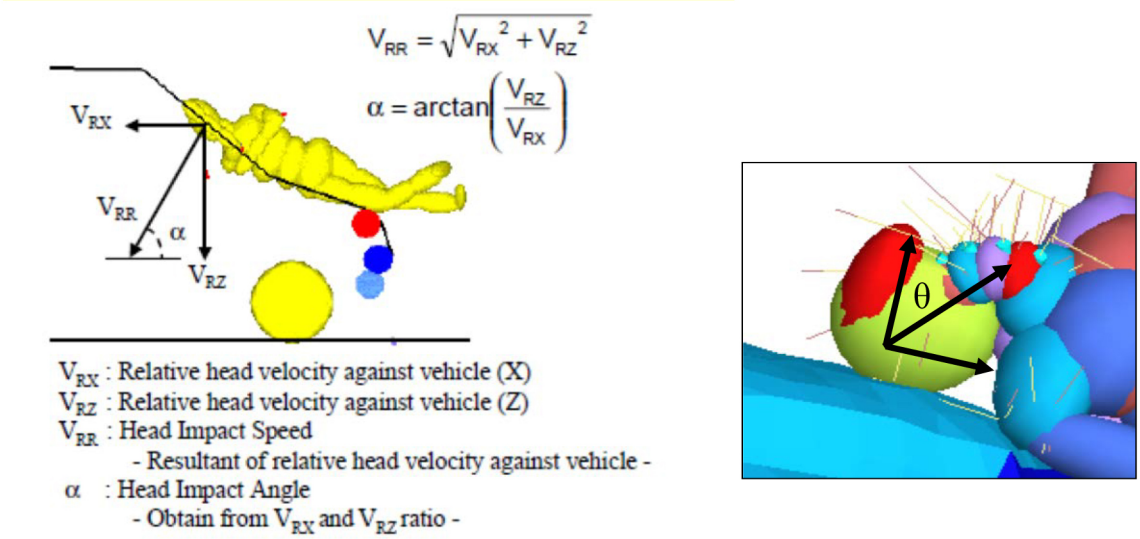

Figure 8. Definitions of Head Contact Velocity, Approach Angle, and Tangential/Normal Angle

Table 4. Summary of Sensitivity Study

Vehicle Speed (km/hr)	Relative Bumper-to-Knee Height	Head Contact Velocity* (km/hr)	Head Approach Angle α* (deg)	Avg θ (Tan^{-1} (Tangential Force/Normal Force))	HIC 15	CSDM	DDM	RMDM
18	-5 cm	25.3	15	54.20	199	0.068	0.021	2.31
24	Baseline	26.7	7	55.51	114	0.189	0.017	1.95
24	+5 cm	30.7	22	2.69	118	0.131	0.003	0.97
24	-5 cm	31.9	50	10.39	1015	0.779	0.008	4.82
32	Baseline	41.0	25	49.30	771	0.753	0.017	4.11
32	+5 cm	41.6	30	45.21	731	0.771	0.014	4.44
32	-5 cm	38.3	22	51.68	510	0.566	0.013	3.68

**Head approach angle is relative to ground; head contact velocity is relative to vehicle*

Table 5. Results from Multiple Regression (* Indicates Statistical Significance, p < 0.05)

Regression Equation	R-Squared	P-Values		
		Head Contact Velocity	Head Angle	Average Theta
HIC = - 953 + 21.2 Velocity + 18.8 Angle + 6.09 Theta	0.975	0.028*	0.006*	0.036*
CSDM = - 1.09 + 0.0317 Velocity + 0.0114 Angle + 0.00466 Theta	0.960	0.013*	0.032*	0.092
DDM = 0.00330 + 0.000145 Velocity - 0.000263 Angle + 0.000254 Theta	0.922	0.425	0.044*	0.015*
RMDM = - 3.57 + 0.107 Velocity + 0.0544 Angle + 0.0404 Theta	0.994	0.002*	0.002*	0.001*

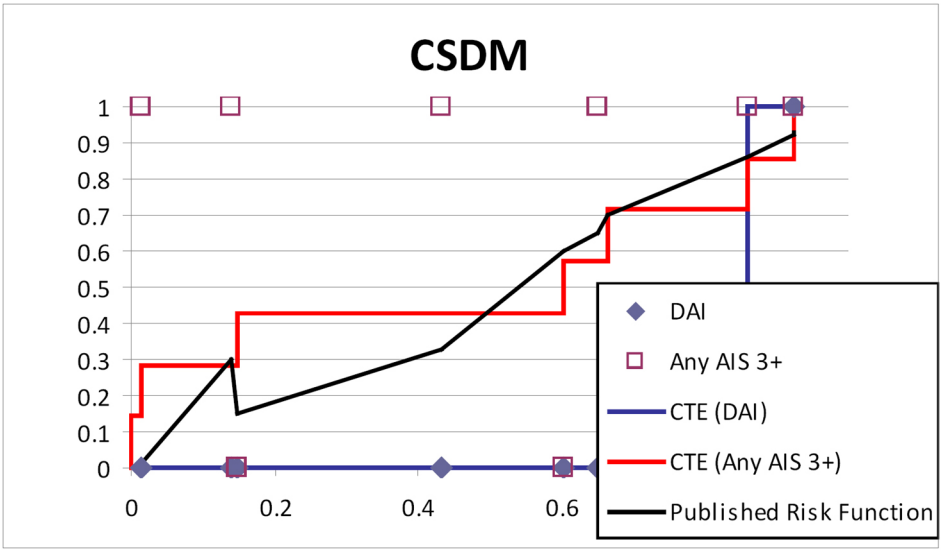

Figure 9. Consistent Threshold Analysis for CSDM

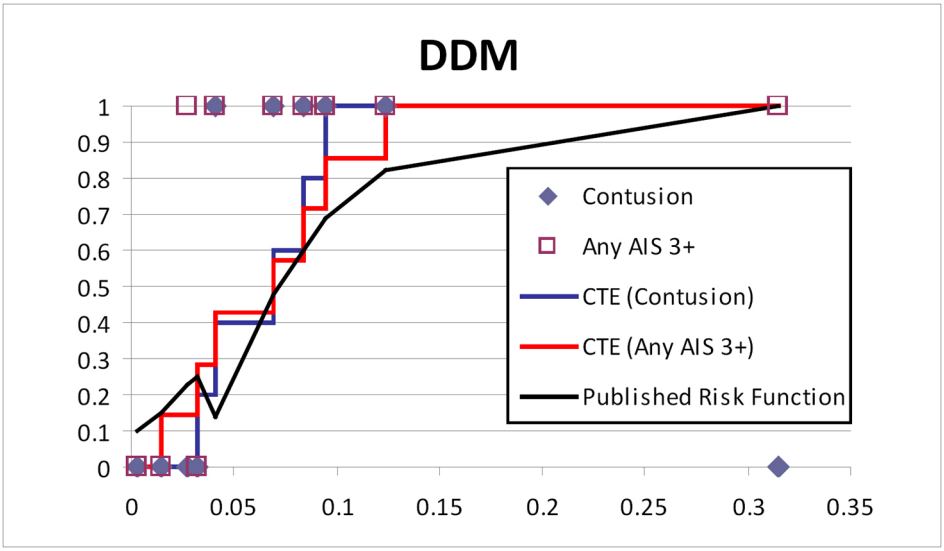

Figure 10. Consistent Threshold Analysis for DDM

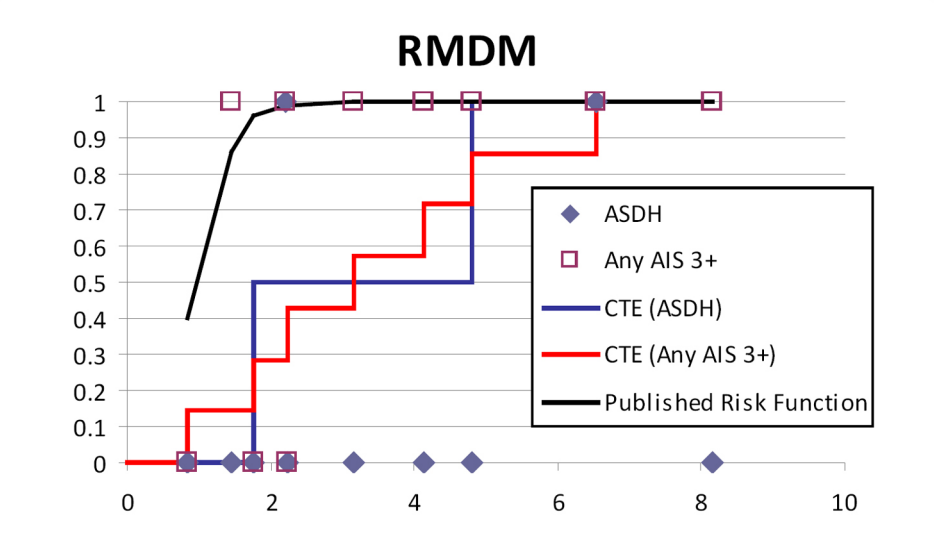

Figure 11. Consistent Threshold Analysis for RMDM

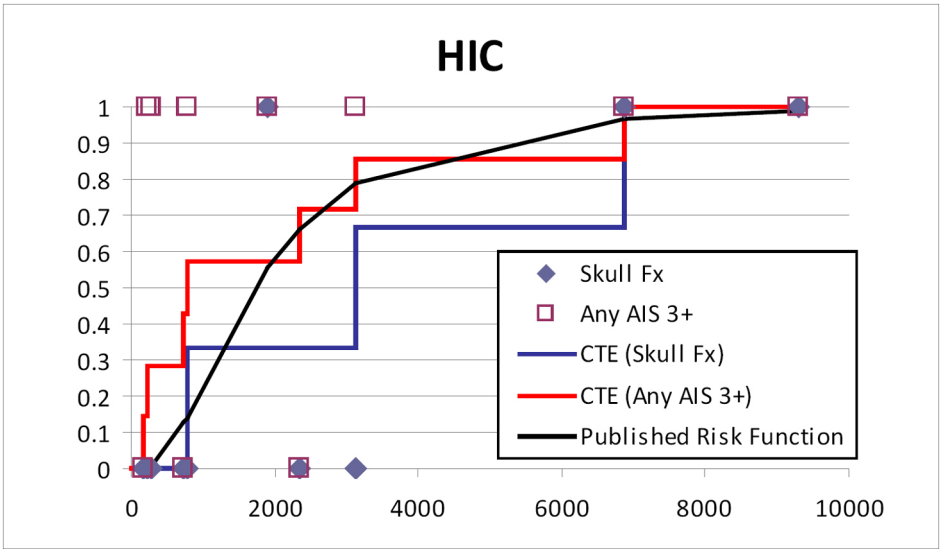

Figure 12. Consistent Threshold Analysis for HIC